nature reviews urology

https://doi.org/10.1038/s41585-025-01111-w

Review article

Check for updates

Micro-ultrasound for prostate cancer

Melis Guer[1,2], Wayne G. Brisbane[3], Hannes Cash[4], Sangeet Ghai[5], Laurence Klotz[6], Paul F. R. Wilson[7] & Adam Kinnaird[1,8]

Abstract

The diagnostic workflow for prostate cancer detection has evolved substantially with advances in imaging technologies and biopsy techniques. Currently, MRI is the standard modality for prostate imaging in cancer detection. However, the rising incidence of prostate cancer and the limited accessibility and high cost of MRI created a growing need for more cost- and time-effective alternative imaging modalities. Micro-ultrasound (microUS), which enables prostatic ductal anatomy to be imaged with a 70-micron resolution, provides an alternative. Level 1 evidence currently shows the non-inferiority of microUS in detecting Grade Group ≥2 prostate cancer in biopsy-naive men compared with MRI. Clinical trials are ongoing to investigate microUS in various other indications. Inter-reader variability needs to be optimized, possibly through the incorporation of artificial intelligence (AI) assistance.

Sections

[1]Division of Urology, Department of Surgery, University of Alberta, Edmonton, Alberta, Canada. [2]Department of Urology, University Hospital Tübingen, Tübingen, Germany. [3]Department of Urology, University of California Los Angeles, Los Angeles, CA, USA. [4]PROURO, Berlin, Germany, Department of Urology, University Clinic for Urology, Urooncology, Robot-assisted and Focal Therapy, University Clinic of Magdeburg, Magdeburg, Germany. [5]University Medical Imaging Toronto, Joint Department of Medical Imaging, University Health Network-Mount Sinai Hospital-Women's College Hospital, University of Toronto, Toronto General Hospital, Toronto, Ontario, Canada. [6]Division of Urology, Sunnybrook Health Sciences Center, Toronto, Ontario, Canada. [7]Queen's University, Kingston, Ontario, Canada. [8]Department of Oncology, University of Alberta, Edmonton, Alberta, Canada. e-mail: ask@ualberta.ca

Key points

- High-resolution micro-ultrasound (microUS) is a new imaging technology for prostate biopsy that has a resolution of 70 microns.
- The OPTIMUM randomized controlled trial provided level 1 evidence that microUS is non-inferior to MRI for the detection of Grade Group 2 or higher prostate cancer in biopsy-naive men.
- Artificial intelligence based on microUS imaging features is being used to develop models that estimate risk of prostate cancer to assist with targeted prostate biopsy.
- Several prospective multicentre trials (MUSIC-Screen and MUSIC-AS) are under way to determine whether microUS is non-inferior to MRI in biopsy decision-making and active surveillance.

Introduction

Prostate cancer diagnosis has evolved through multiple imaging technologies and biopsy techniques. Prostate biopsy has been carried out since the early twentieth century, beginning with open perineal approaches followed by transrectal and transperineal finger-guided techniques using core needles[1–6]. Conventional transrectal ultrasound (TRUS)-guided biopsy, initially introduced for prostate evaluation in 1963, gradually replaced the finger-guided technique[7]. TRUS became reliable for prostate cancer diagnosis in the 1980s, with the introduction of improved probes and the development of an attachable biopsy needle guide[8,9]. However, conventional TRUS distinguishes zonal anatomy of the prostate, but fails to visualize most prostate cancers.

In the late 1980s and 1990s, MRI was first used for prostate imaging, although it was limited by poor resolution and diagnostic criteria[10]. The development of multiparametric MRI (mpMRI) improved detection of prostate cancer and enabled targeted biopsies, including cognitive, in-bore and MRI–TRUS device-based fusion techniques[11]. mpMRI was standardized by the Prostate Imaging Reporting and Data System (PI-RADS) in 2012, with iterative versions in 2015 and 2019 (ref. 12), and recommended by major international guidelines such as those of the European Association of Urology and American Urology Association for pre-biopsy evaluation[13,14]. However, mpMRI still can miss ≥15% of clinically significant prostate cancers, defined as Gleason Grade Group (GG) ≥2[15,16]. Furthermore, MRI wait times are in the order of multiple months in publicly funded health care systems, and MRI requires sophisticated imaging facilities that are rarely found in rural hospitals and developing nations.

Another imaging technology for prostate cancer is PET with prostate-specific membrane antigen ligands. This technique has been used in both staging and biopsy settings[17,18]. However, similarly to MRI, the broad implementation of prostate-specific membrane antigen PET is limited by the need for advanced imaging facilities, cost and the duration of the scans.

The 29-MHz high-resolution micro-ultrasound (microUS) imaging platform was first introduced in the mid-2010s as an alternative modality to MRI for prostate cancer detection. The 29-MHz microUS device — commercially available as the ExactVu system — has a 70-µm resolution, which enables this system to operate at high frequencies and to provide an increased imaging depth of the prostate, resulting in improved visualization of prostate lesions. In a 2025 multicentre international randomized controlled trial, microUS-guided biopsy was shown to be non-inferior to MRI-guided biopsy in detecting clinically significant prostate cancer[19]. Importantly, this technology also addresses several crucial limitations associated with MRI-guided biopsy, including high costs, limited scanner availability, prolonged waiting times, susceptibility to motion and image artefacts and disparities in access across different health care settings, while offering a promising solution for MRI-ineligible patients, such as those with contrast agent allergies or ferromagnetic implants.

Technical overview

Advances in miniaturization of ultrasound arrays have enabled clinically useful microUS to be created, with higher frequency and tighter crystal packing than previously possible. In the case of ExactVu (the only commercially available microUS device), 512 individual crystal elements are packed with a spacing of 90 µm, providing sufficient density to eliminate grating lobe artefacts at the higher frequencies required for microUS imaging. These crystals are made to provide extremely wide bandwidth and low crosstalk, enabling the high sensitivity and deep imaging level to be reached that are required for the prostate (Fig. 1).

ExactVu microUS was developed to provide a 70-µm resolution, which is required to properly image prostatic ductal anatomy, as prostate ducts have an average size of 100 µm in healthy tissue. Disruptions in the normal ductal architecture are used to grade cancer in histopathology samples. A frequency of 29 MHz was selected for this system to balance the required resolution with the required imaging depth. In combination with advanced signal processing and precise transmit-receive protocols, this system can provide the required 70-µm resolution along with a 6-cm image depth (which is satisfactory for most prostate sizes). Additionally, in 2019, a software-based fusion function (FusionVu) was integrated into microUS, leading to the integration of MRI data into real-time microUS-guided fusion biopsies (known as microUS/MRI fusion).

Preclinical and clinical developments of microUS

The evolution of high-frequency microUS began in the late 1980s with the first non-invasive imaging of tumour spheroids at 100 MHz[20], leading to early clinical applications in ophthalmology[21,22], dermatology[23,24] and intravascular imaging[25,26]. The use of microUS in preclinical imaging of embryonic mouse development was also initiated in 1995 (ref. 27). Subsequently, diverse systems and applications were developed across multiple fields[28,29], including the introduction of a commercially available transducer-based microUS imaging system in 2009 (15–50 MHz), which enabled real-time visualization of embryonic development and blood flow in mouse models of tumour angiogenesis[30] (Fig. 2).

The application of high-frequency microUS in preclinical cancer studies in liver metastasis and transgenic prostate cancer mouse models enabled precise monitoring of tumour volume changes associated with tumour progression[31,32]. Additionally, microUS has been used to visualize the tumour vascularization in a genetically engineered mouse model of prostate cancer[33], and to assess the efficacy of antiangiogenic therapeutics in a human breast cancer xenograft mouse model[34]. Specifically for the prostate, in 2005, microUS was used to track 3D tumour volume in a transgenic prostate cancer mouse model[31]. In 2007, power Doppler was added to microUS imaging to depict functional neoangiogenic blood flow in prostate tumours compared with normal prostate tissue[33].

The first-generation microUS system in clinical use for prostate cancer detection was initially evaluated in a 2014 pilot study using

radical prostatectomy specimens. MicroUS showed superiority over conventional (5 MHz) US in visualizing tumours, showing improved sensitivity (65.2% versus 37.7%) and specificity (71.6% versus 65.4%) ($P = 0.006$)[35]. Subsequently, several prospective and retrospective series have been initiated to integrate microUS into the prostate biopsy procedure. In 2020, microUS was evaluated in comparison with conventional-frequency (5–12 MHz) TRUS-guided biopsy in a randomized controlled trial. In this study, the per-patient detection rates of clinically significant prostate cancer did not differ between transrectal micro-US and conventional-US arms (34.6% versus 36.6%, respectively, $P = 0.21$)[36]. Additionally, microUS has been investigated in multiple observational studies, in which microUS was compared with MRI-TRUS fusion biopsy. Although methodological differences existed across these studies, results from these trials showed improved detection rates of clinically significant prostate cancer with microUS, suggesting microUS as a potential imaging modality for targeting prostate lesions[37,38].

MicroUS in the diagnosis of prostate cancer

The diagnostic accuracy of microUS for GG ≥2 prostate cancer has been evaluated in several clinical studies involving patients with suspected prostate cancer. The earliest registration study was conducted in 2020 and involved a large cohort of 1,040 patients undergoing various biopsy protocols. In this study, a sensitivity of 94% and a negative predictive value (NPV) of 85% were reported, both comparable to those obtained with MRI (sensitivity 90%, $P = 0.03$; NPV 77%)[39]. Early results from a single-institutional prospective study including 320 men showed a sensitivity of 90%, with a NPV of 82% for microUS[40]. The updated analysis of this study in an expanded cohort of 1,423 men showed a sensitivity of 85% and a NPV of 79% in detecting GG ≥2 prostate cancer[41]. Notably, in this study, GG ≥2 was detected through microUS-targeted biopsy in 419 of 871 men who had a negative MRI-targeted biopsy, whereas MRI-targeted biopsy identified GG ≥2 in 66 of 529 men with a negative microUS-targeted biopsy. These findings indicate that microUS seems to provide additional information and can enhance the detection of clinically significant prostate cancer when combined with MRI in a single biopsy procedure[41]. In another study including 159 patients with MRI-detected lesions scored as PI-RADS ≥3, micro-US-targeted biopsies showed a higher International Society of Urological Pathology grade group than non-targeted biopsies in 26% of patients (42 of 159) and higher than both non-targeted and MRI-targeted biopsies in 16% (26 of 159). Overall, microUS-targeted biopsy resulted in a pathological upgrade in 9.4% more patients than MRI-targeted biopsy ($P = 0.005$)[42]. Results from a prospective study including 203 patients showed non-inferiority of microUS to MRI in detecting GG ≥2 tumours[43]. In another prospective study including 94 patients, comparable GG ≥2 detection rates were observed between microUS and mpMRI targeted biopsy (35% versus 39%)[44]. Results from a study including 111 patients with PI-RADS ≥3 lesions showed high sensitivity and NPV (100%) of microUS in detecting GG ≥2, whereas specificity and positive predictive value were 33.7% and 27.2%, respectively[45].

Results from studies in which microUS-guided biopsy was used in biopsy-naive men with a negative MRI — defined by a PI-RADS score of ≤2 — showed that some lesions were visualized by microUS but not MRI[46,47]. Furthermore, results from a prospective trial including 425 men who underwent prostate cancer screening showed that men with a Prostate Risk Identification using Micro-UltraSound (PRI-MUS, a structured scale that ranges from 1 to 5, indicating the likelihood of cancer detection) score ≤2, had improved biopsy-free survival (HR 0.17; $P < 0.001$), cancer-free survival (HR 0.12; $P < 0.001$) and clinically significant cancer-free survival (HR 0.09; $P < 0.001$) compared with those who had a PRI-MUS score ≥ 3 (ref. 48). Results from this study suggest a potential use of the PRI-MUS score to refine patient risk stratification for prostate cancer screening, aiming to reduce unnecessary work-up[48].

In the phase III, prospective, open-label, non-inferiority OPTIMUM clinical trial, 802 patients were randomized in a 1:2:3 ratio to

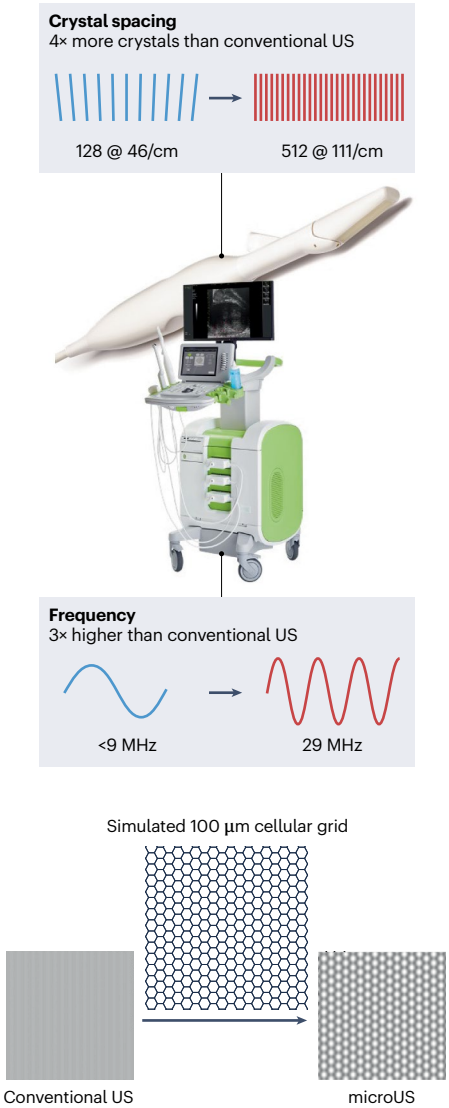

Fig. 1 | Technical overview of micro-ultrasound. The micro-ultrasound (microUS) device is shown with highlighted technical features that differentiate this device from conventional ultrasound (US). Specifically, microUS operates at a frequency of 29 MHz, which is approximately three times higher than conventional US (<9 MHz). In terms of crystal spacing, microUS probes contain 512 crystals arranged at 111 crystals/cm, compared with 128 crystals at 46 crystals/cm in conventional US, enabling the high sensitivity and deep imaging level to be reached that are required for the prostate. The higher frequency and denser crystal configuration of microUS enable a spatial resolution of ~70 µm to be reached, providing more detailed tissue characterization than that obtained with conventional US. Device image courtesy of Exact Imaging.

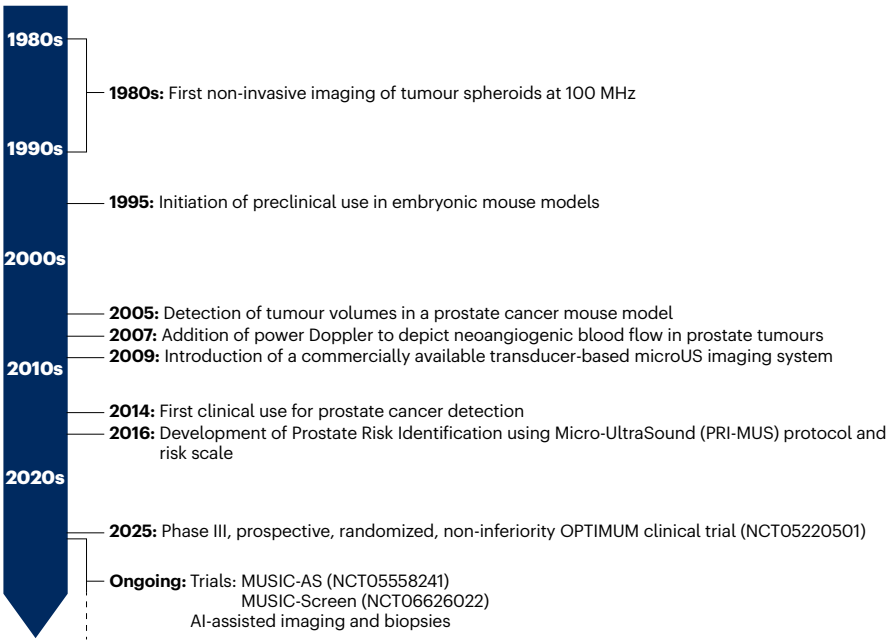

Fig. 2 | Timeline of the development and implementation of micro-ultrasound. Timeline illustrating crucial milestones in the preclinical development, validation and clinical implementation of micro-ultrasound from the 1980s to 2025, including ongoing trials.

microUS-guided biopsy, combined MRI/microUS fusion-guided biopsy, and software-assisted MRI plus conventional US fusion-guided biopsy at 20 centres in eight countries. Results from this pivotal trial showed that microUS and combined MRI/microUS fusion-guided biopsy were non-inferior to MRI plus conventional ultrasonography fusion-guided biopsy for the detection of GG ≥2 tumours in biopsy-naive men (absolute difference between microUS and MRI + conventional US: 4 (95% CI −4 to 11), $P < 0.001$; absolute difference between MRI/microUS and MRI + conventional US: 4 (95% CI −4 to 13), $P < 0.001$). The detection of GG 1 prostate cancer was comparable between the groups (11.6%, 15.4% and 17.3% in the microUS, MRI plus conventional US, and MRI plus microUS fusion-guided biopsy groups, respectively; one-way ANOVA $P = 0.37$). Excluding systematic samples, the targeted-only detection rates of microUS-guided biopsy and combined MRI/microUS fusion-guided biopsy were also non-inferior to MRI plus conventional US fusion-guided biopsy (absolute difference between microUS and MRI + conventional ultrasonography: 4 (95% CI −6 to 14), $P < 0.002$; absolute difference between MRI/microUS and MRI + conventional ultrasonography: 6 (95% CI −2 to 14), $P < 0.001$). A limitation of this trial was the mandatory systemic biopsy for all men, regardless of microUS and MRI findings and PSA density; in current practice, systematic biopsies are often avoided[19].

The important clinical implication of these non-inferiority results is the potential introduction of a single-encounter biopsy procedure through microUS, with many potential benefits. These benefits include the absence of a requirement for contrast medium, no contrast-related morbidity, reduced waiting times, improved patient convenience, and reduced cost and patient anxiety. Considering the anticipated growing disparity between the growth in prostate cancer incidence and the available MRI capacity, microUS might improve diagnostic access for prostate cancer detection[49] (Table 1). The ExactVu is FDA 510k cleared in the USA and is reimbursed by using existing Current Procedural Terminology codes. Globally, the system is widely commercially available in>60 countries.

Diagnostic accuracy of microUS versus MRI for prostate cancer on prostatectomy specimens

Prostatectomy specimens with whole-mount histopathology have been examined in several studies to compare the diagnostic accuracy of microUS and MRI. In a retrospective study of 65 prostatectomy specimens, microUS contiguous para-sagittal images were converted into a 3D model to predict the pathological tumour volume[50]. A total of 104 lesions were identified through whole-mount histopathology, with 84% harbouring GG ≥2 tumours. Median tumour size was 1.05 ml on microUS, 0.73 ml on MRI and 1.2 ml on final pathology. These results underscore the potential underestimation of the real tumour size with both microUS and MRI[50].

In a prospective validation paired-cohort trial (NCT04299620), a multistep methodology that co-registers microUS and MRI findings with whole-mount pathology was developed and assessed in patients undergoing radical prostatectomy[51]. In this trial, microUS had an equivalent performance to that of MRI for index lesion detection (91.7% versus 80%), with higher detection of tumour extent (52.5% versus 36.7%) and a comparable rate of false-positive regions of interest (38.3% versus 40.8%)[51], indicating that microUS offers similar imaging accuracy to MRI for prostate cancer.

Overall, results from whole-mount pathology studies showed that microUS can be a reliable imaging modality with a similar diagnostic performance to MRI in detecting index tumour location, and also in precisely measuring tumour volume, underscoring microUS potential use in presurgical evaluation.

Prostate Risk Identification using Micro-UltraSound risk identification protocol

The PRI-MUS protocol and risk scale was developed in 2016 using the ExactVu microUS system cine loops of 400 biopsies collected as part of a multi-institutional randomized clinical trial, and was validated in an independent, pathology-blinded set of 100 cines[52]. The PRI-MUS score is a structured scale that ranges from 1 to 5, with a lesion with

PRI-MUS score of 1 indicating the lowest risk, and a score of 5 indicating the highest risk of prostate cancer[52] (Fig. 3). In the OPTIMUM trial, no patient with a PRI-MUS score of 1 was diagnosed with a GG ≥2 lesion. For PRI-MUS scores of 1 and 2, the NPV was 83%. Fewer than 10% of biopsies with a PRI-MUS score of 5 showed only GG 1 tumours, whereas 86% of men with a PRI-MUS score of 5 were diagnosed with GG ≥2 lesions[19]. Thus, the PRI-MUS scoring system seems to be effective at differentiating clinically significant prostate cancer from benign tissue. However, updated versions of PRI-MUS will probably continue to enhance microUS-guided biopsy decision making, analogous to iterative versions of PI-RADS.

The PRI-MUS anterior score was developed to predict the likelihood of GG ≥2 lesions in the anterior zone. This score was established by using 102 selected prostate scans through a process that included a development phase — in patients who had undergone radical prostatectomy — and a validation phase — in a separate cohort of patients undergoing microUS-guided prostate biopsy. The PRI-MUS anterior score enables high-risk and low-risk features to be identified, in turn leading to a standardized whole gland assessment when combined with the standard PRI-MUS score[53]. However, several factors — such as the heterogeneous appearance of the transition zone, artefacts from periurethral calcifications and corpora amylacea, and overall signal attenuation at greater tissue depths — might cause lesions in the anterior prostate to be missed[54,55].

Performing a targeted micro-ultrasound biopsy

The ideal number of targeted cores for a microUS-guided biopsy remains undetermined. Results from MRI studies suggest that a range of 2–5 MRI-fusion-guided cores should be sampled per lesion owing to registration error[56]. MicroUS overcomes the registration error associated with MRI fusion devices owing to the real-time visualization of the biopsy needle transgressing the PRI-MUS 3–5 lesions. In a retrospective study, detection rates of clinically significant cancers increased with each cumulative core as the number of microUS-guided cores per lesion increased, to at least three[57]. This result is coherent with the OPTIMUM trial design, which required three targeted cores per lesion.

Inter-observer variability and learning curve

Cancer detection rates of a real-time imaging technology such as microUS are strongly associated with the physician's interpretation, as effective training and quality assurance are essential for the successful clinical implementation of this technology.

The inter-reader agreement on microUS interpretation has been initially evaluated in a multi-reader study by using precise volumetric analysis of lesion overlap on digital annotations[55]. Readers' experiences ranged from 2 to 6 years. No correlation was observed between readers' experience level and inter-reader agreement (κ = 0.30). The chance that two separate readers agreed on the location of a lesion was ~ 30% (positive percentage agreement = 33%)[55]. Additionally, a

Table 1 | Studies comparing microUS and MRI for prostate cancer diagnosis

Year	Number of patients	Design	Detection of GG≥2 lesions	Ref.
2020	1,040	Prospective multicentre registry study for microUS biopsy for patients who received prior mpMRI	MicroUS vs mpMRI: Sensitivity 94% vs 90%, (*P*=0.03) NPV 85% vs 77%	39
2021	320	MicroUS to identify targets with blinded MRI before microUS/MRI ExactVu fusion biopsy	MicroUS: sensitivity 89.7%; NPV 81.5% Sensitivity (PRI-MUS vs PI-RADS): (62.1% vs 65.5%) for Score 5 (39.6% vs 33.0%) for Score 4 (13.2% vs 19.3%) for Score 3	40
2021	159	MicroUS to identify targets with blinded MRI	7% (27 of 159) of patients with a negative mpMRI targeted biopsy had a positive microUS-targeted biopsy; 7 patients had clinically insignificant prostate cancer, whereas 20 patients had GG≥2 cancer	42
2021	111	MicroUS to detect clinically significant prostate cancer in patients with a PI-RADS 3 lesion at MRI	MicroUS: sensitivity 100%; NPV 100%; specificity 33.7%; PPV 27.2%	45
2022	203	Non-inferiority analysis of microUS (with blinded MRI) vs MRI-TRUS fusion biopsy in the same procedure	MicroUS was non-inferior to mpMRI-TRUS fusion biopsy	43
2022	94	MicroUS-targeted biopsy, followed by completion of additional targets identified through unblinded MRI+systematic biopsy	GG≥2 lesion rate was comparable between microUS- and mpMRI-targeted biopsy (35% vs 39%)	44
2023	125	MicroUS-guided biopsy in biopsy-naive patients with negative MRI	Micro-US: sensitivity 97.1%; NPV 96.4%; specificity 29.7%; PPV 34.0%	47
2024	103	MicroUS-guided biopsy in biopsy-naive patients with negative MRI	PSA density<0.15 and PRI-MUS≤2: 14% PSA density≥0.15 and PRI-MUS≥3: 60% (*P*=0.02)	46
2025	425	MicroUS assessment to optimize diagnostic work-up	Men with PRI-MUS score≤2: biopsy-free survival HR 0.17; cancer-free survival HR 0.12; clinically significant cancer-free survival HR 0.09 (*P*<0.001)	48
2025	1,423	Updated results of[40]	MicroUS: sensitivity 85%; NPV 79%	41
2025	802	1:2:3 randomization to microUS, microUS/MRI, and MRI+conventional US	MicroUS and microUS/MRI were non-inferior to MRI+conventional US	19

GG, Gleason Grade Group; HR, hazard ratio; microUS, micro-ultrasound; NPV, negative predictive value; PI-RADS, Prostate Imaging Reporting and Data System; PPV, positive predictive value; PRI-MUS, Prostate Risk Identification using Micro-UltraSound.

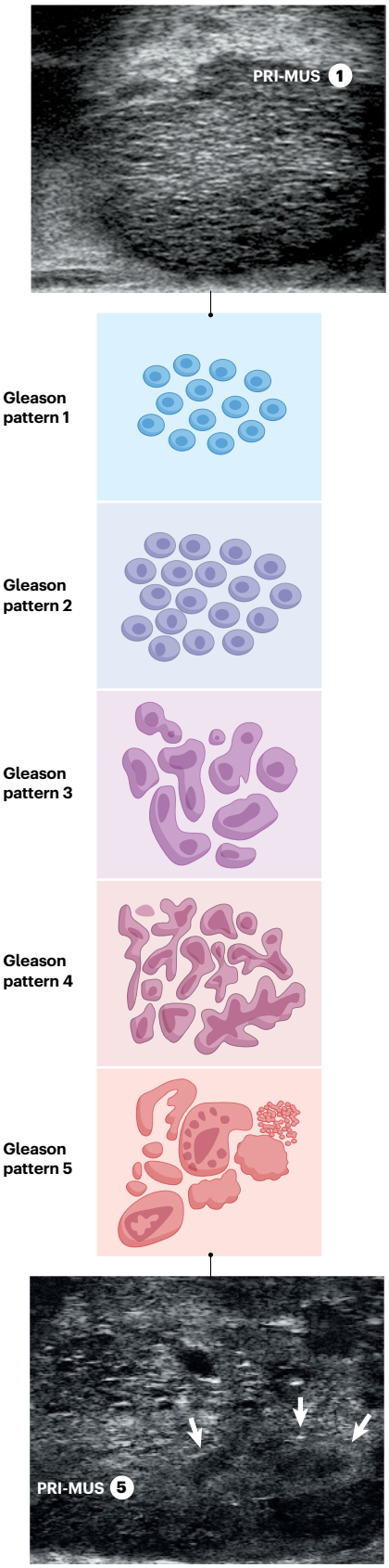

Fig. 3 | Gleason patterns in ductal architecture detected through micro-ultrasound and scored through Prostate Risk Identification using Micro-UltraSound. The correlation between micro-ultrasound (microUS) imaging features and histopathological Gleason grading is shown. Top panel: example of a Prostate Risk Identification using Micro-UltraSound (PRI-MUS)-1 microUS image of the prostate, consistent with benign tissue. Middle panel: schematic representation of Gleason patterns 1–5, depicting the progressive glandular disorganization and increased tumour aggressiveness. Bottom panel: example of a PRI-MUS-5 microUS image of the prostate, with white arrows delineating the tumour lesion boundaries.

reader sensitivity of 0.66 was observed in this study, probably as a consequence of a high prevalence of anterior prostate lesions. Excluding anterior lesions resulted in an increase in mean reader sensitivity (from 0.66 to 0.87) and in positive percentage agreement (from 29% to 43%)[55]. Furthermore, increased reader agreement was observed for high-grade prostate cancer detection, with readers being more than 12 times more likely to detect GG ≥3 than GG 2 cancers (mean reader sensitivity of 0.88)[55].

In 2018, Exact Imaging (the company that sells the ExactVu microUS device) launched a voluntary, comprehensive training programme to improve the learning curve in microUS-guided biopsy. The programme includes four scheduled feedback stages. Novice users are required to achieve specific scores on nine biopsy quality metrics — selected from the first microUS-based randomized trial — to progress to the next stage[52]. The effect of this training programme on the detection rate of GG ≥2 lesions was retrospectively evaluated, showing a 17% increase in detection effectiveness[58]. This increase in cancer detection was noted after feedback was given on 40 procedures (at the third stage) and persisted after feedback on 90 procedures (at the fourth stage), suggesting that the learning curve is ~40 procedures. MicroUS is a relatively new technology; thus, no large "real world" data are currently available. However, as per our understanding, training sessions are provided by the vendor at no charge, and most centres in which this technology is used are undertaking this training opportunity.

Role of micro-ultrasound for active surveillance

Active surveillance (AS) has emerged as standard-of-care for men with low-risk prostate cancer. AS limits risks of sexual, urinary and bowel function compared with surgery or radiation. The decision to enter AS rather than undergo treatment is primarily based on tumour aggressiveness. Thus, accurate assessment is crucial to avoid missing high-risk tumours that can become lethal if not treated. During AS, patients undergo serial imaging and histopathology assessments over time.

In a feasibility study with a limited cohort including nine patients undergoing AS, microUS detected 89% of clinically significant cancers compared with 56% for MRI[59]. In a prospective study including 100 patients undergoing AS, microUS and MRI showed sensitivities of 94.1% and 100% for the detection of GG ≥2 prostate cancer, and NPVs of 88.9% and 100%, respectively[60]. Preliminary evidence on the use of microUS for AS has showed similar results to MRI in detecting GG ≥2 prostate cancer, underscoring the feasibility of microUS as an imaging tool as well as real-time guidance of targeted and systematic biopsy samples[59,60].

Surveillance biopsy to detect pathological upgrading is crucial for the decision to switch to active treatment. In a study including 128 patients diagnosed with GG 1 prostate cancer, no significant difference ($P = 0.22$) was observed between MRI and microUS in detecting GG ≥2 lesions. Interestingly, when microUS and MRI were combined,

no instances of upgrading were observed in patients with negative findings on both scans, introducing a provocative concept of a biopsy-less surveillance method[61]. Overall, microUS seems to provide similar imaging data to MRI in patients on AS. However, additional clinical trials are needed to achieve level 1 evidence.

Micro-ultrasound for prostate cancer tumour staging

MicroUS offers a promising alternative imaging modality for local tumour staging. MicroUS has been shown to be effective in detecting extraprostatic extension (EPE), defined as the presence of either extracapsular extension (ECE) or seminal vesicle invasion (SVI), which can substantially influence surgical planning[62,63]. Morphological features of extraprostatic extension that have been observed through microUS include a visible breach of the prostate capsule, capsular irregularity or bulging, obliteration of the prostatic–seminal vesicle angle, and the presence of a hypoechoic halo[64].

In a feasibility study of microUS for detecting EPE including 54 patients with prostate cancer before radical prostatectomy, ECE, a capsular bulge and a hypoechoic halo detected through microUS were significantly more prevalent in patients with non-organ-confined disease ($P \leq 0.016$), indicating that microUS can serve as a useful tool for preoperative risk stratification and optimization of the surgical approach[62]. Similarly, in a prospective trial including 140 patients with prostate cancer who underwent surgery, microUS findings had an NPV of 80.5% and a positive predictive value of 83.0% for ECE, with an area under the curve of 80.4%[63]. However, current guidelines recommend MRI for preoperative local staging[14], and head-to-head comparator studies are required to assess MRI versus microUS in prostate cancer staging.

Micro-ultrasound for prognosis

Radiogenomic analysis of MRI visibility has shown that genetic alterations associated with MRI visibility are the same alterations that drive tumour aggressivity. Conversely, MRI-invisible lesions lack these alterations, conferring an indolent phenotype in most instances[65]. Thus, MRI invisibility is a powerful prognostic tool. Whether microUS invisibility or other imaging characteristics have the same association with favourable genomics is not known, and studies to assess the genomics of microUS-visible versus microUS-invisible cancers will be needed to address this unmet need.

Micro-ultrasound in focal therapy

An advantage of microUS is real-time lesion localization, which, during biopsies, permits the direct visualization of a biopsy needle transgressing the region of interest. This concept has been applied to focal therapy, including cryoablation and focal laser ablation[66,67]. Results from several series showed the feasibility of placing the ablative cryoablation needle or laser fibre directly into the tumour. Furthermore, live thermal ablation of tissue by using microUS has been described, and enabled to determine treatment margins in real time[66]. The utility of microUS for follow-up monitoring post-ablation remains to be determined.

Artificial intelligence and micro-ultrasound

Artificial intelligence (AI) is being investigated to standardize microUS interpretation, reduce inter-reader variability and support real-time decision making during biopsy. Crucial development areas in this field are prostate segmentation, image classification and lesion detection.

In 2024, a deep-learning-based AI tool, MicroSegNet, was introduced for automated prostate segmentation on microUS images[68]. This tool enables the prostate capsule to automatically be identified on microUS images, providing a crucial first step for AI-based cancer detection in the prostate. In a study in which MicroSegNet was assessed by using microUS images from 55 patients for training and images from an independent set of 20 patients for validation, MicroSegNet achieved a Dice coefficient of 0.939, showing superior performance compared with several segmentation methods and expert reviewers[68].

A multi-scale deep-learning model, TRUSformer, was proposed to classify microUS images as cancerous or benign. This model used a hybrid network architecture consisting of a self-supervised convolutional network and a transformer network. TRUSformer achieved 88% sensitivity and 51% specificity on a dataset of 125 patients who underwent systematic TRUS-guided biopsy for suspected prostate cancer[69]. An integrated system, TRUSWorthy, similarly based on self-supervised learning and transformers, was introduced to address the challenges of label scarcity, weak labelling, class imbalance and data heterogeneity in microUS to produce robust prostate cancer classification models[70]. In a co-registration study, a multistep methodology was used to co-register microUS images with whole-mount pathology findings, generating training labels for a cancer classification model[51]. The outputs of this deep-learning model, trained on labelled microUS images, were directly compared with expert microUS reviewers in an exploratory dataset including 15 patients[71]. In this study, the AI model outperformed a novice reviewer and showed similar performance to that of an expert reviewer, with sensitivity of 78.9% versus 60.6% and specificity of 72.7% versus 80.5%, respectively[71].

Promising results in AI-driven prostate cancer detection were obtained with the ProstNFound model, which uses medical foundation models to analyse microUS imaging features together with clinical markers. In a multicentre microUS dataset including 693 patients who underwent microUS-guided prostate biopsy, this model achieved 90% sensitivity and 40% specificity[72]. ProstNFound generates a 'heatmap' of cancer suspicion, which could be used to identify lesions for targeted biopsy (Fig. 4). In a 2025 study, ProMUS-NET (a no-new U-Net model) showed superior accuracy for the detection of GG ≥2 cancers than expert urologists on a per lesion level (lesion-level sensitivity: 73% versus 58%; $P = 0.014$)[73].

AI-based approaches show promising results for improving and standardizing prostate microUS analysis. AI models could improve cancer detection and identification of locally advanced disease, while also reducing inter-observer variability. Furthermore, generating an AI-driven 3D model of the prostate and tumour lesions by using microUS imaging data might provide additional value in planning focal therapy for localized prostate cancer. Small sample size is currently a major limitation to AI experiments using microUS images. Large numbers of patients will be required for the validation of these novel AI tools, and current efforts are underway to centralize deidentified microUS images from multiple multicentre trials.

Other indications for micro-ultrasound

The high resolution of microUS with improved real-time visualization of tissue details opens to application for various clinical settings such as bladder cancer, male factor infertility and urethral stricture. For example, in two prospective studies, microUS showed feasibility and effectiveness in the detection and staging of bladder cancer. In a feasibility study including 23 patients with bladder cancer, microUS identified all non-invasive tumour stages appropriately, whereas tumours in two patients were downstaged following histopathological correlation[74]. In a head-to-head comparison of microUS versus MRI in 58 patients

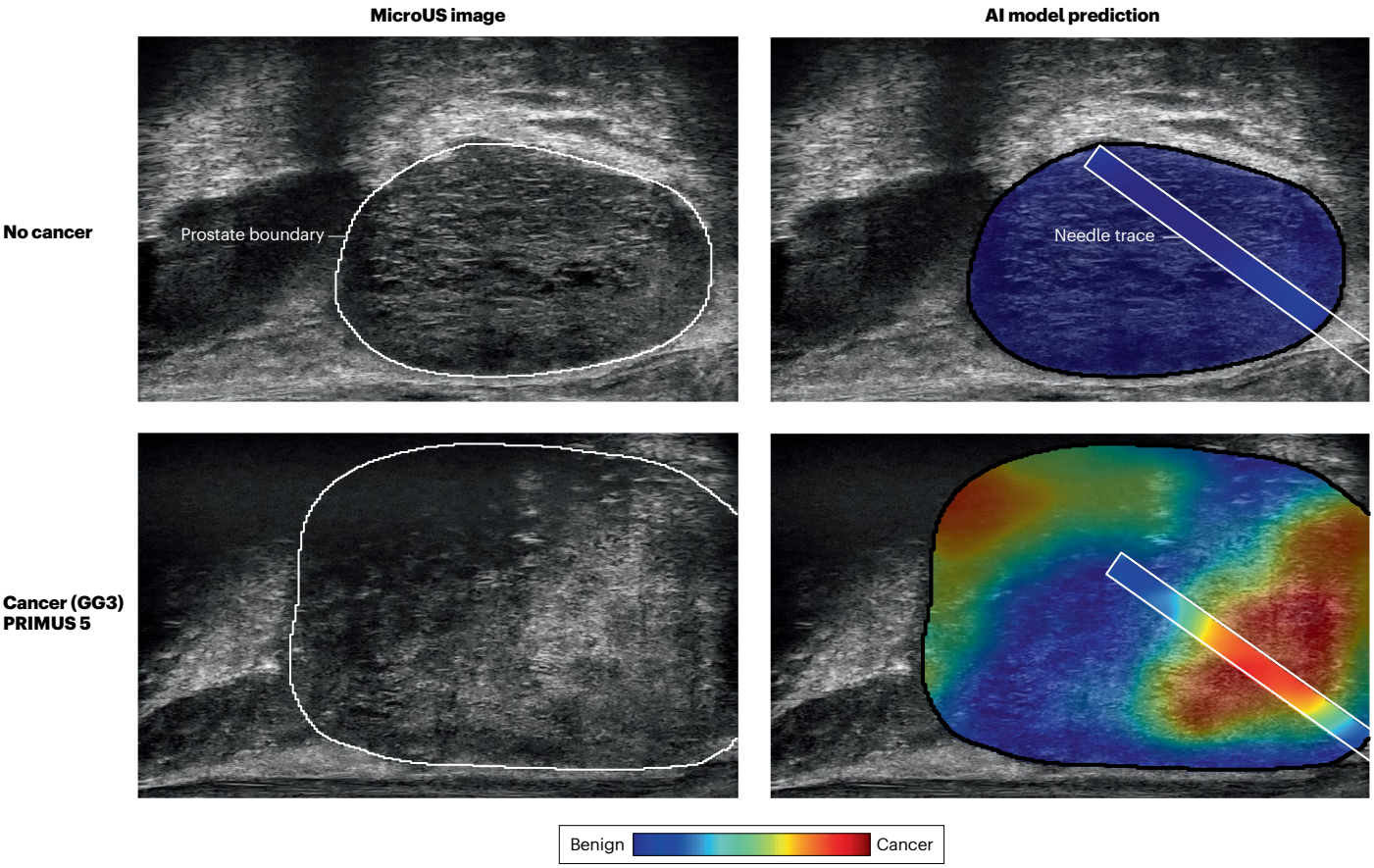

Fig. 4 | Example of artificial intelligence-generated predictions of micro-ultrasound images. Example heat maps generated by using the ProstNFound artificial intelligence (AI) model for micro-ultrasound (microUS) are shown. The top panels show an example of benign prostate imaging on microUS (with benign biopsy histology) and the corresponding 'cold' heatmap, whereas the bottom panels show an example of a Prostate Risk Identification using Micro-UltraSound (PRI-MUS) 5 lesion (with Gleason Grade Group (GG) 3 biopsy histology) and the corresponding 'hot' region of interest on the heatmap.

with bladder cancer, both modalities showed comparable diagnostic accuracy, with identical sensitivity (85%) and similar NPVs (90.6% versus 86.4%), supporting the use of this cost-effective technology in primary diagnosis of bladder cancer[74,75]. However, to date, the limited field of view and the lack of an established scoring system for bladder lesions constrain microUS adoption into clinical practice.

Multiparametric ultrasound techniques have been used for scrotal imaging in the evaluation of infertility[76] and a prospective clinical trial is currently underway to assess the utility of microUS for the detection of azoospermia (NCT06941922)[77]. This study is expected to be completed in December 2025.

Ultrasound of urethral tissue is an emerging method in the diagnosis of urethral stricture, which was shown to be superior to conventional imaging for anterior urethral strictures in several studies[78]. Clinical trials assessing the feasibility of microUS in anterior urethra stricture are currently lacking.

Specifically for the prostate, microUS might assist with preoperative evaluation and treatment decision-making for benign prostatic hyperplasia by providing detailed anatomical insights. However, considering the relatively new development of microUS, to our knowledge, no study has yet been carried out for this indication.

Ongoing micro-ultrasound trials in prostate cancer

The Micro-UltraSound In Cancer-Active Surveillance (MUSIC-AS) trial (NCT05558241) is an ongoing international, multicentre, non-inferiority, prospective paired diagnostic study designed to compare micro-ultrasound and MRI during AS of prostate cancer. In this study, progression to GG ≥ 2 tumour is assessed through a structured biopsy protocol, beginning with micro-US-targeted sampling (carried out by clinicians who are blinded to MRI results), followed by MRI-targeted sampling, and completed with 12 systematic biopsy cores. The primary objective is to evaluate whether micro-US-guided biopsy is non-inferior to MRI-guided biopsy in detecting GG ≥2 cancer at confirmatory biopsy[79].

The MUSIC-Screen trial (NCT06626022) is an ongoing multicentre, international, non-inferiority, randomized clinical trial designed to evaluate whether microUS is non-inferior to the current standard imaging modality — multiparametric MRI — for determining the need for prostate biopsy. Participants in this trial will be randomized into two groups to compare microUS versus MRI results to guide the decision for proceeding to prostate biopsy, with the detection of GG ≥2 lesions as the primary outcome. Participants will be followed for 8 years after

initial imaging to determine how many men in each group were subsequently diagnosed with GG ≥2 cancer. This study is aimed at identifying whether microUS can match the diagnostic accuracy of MRI[80].

A retrospective series (DRKS00036777) including biopsy-naive men from multiple German centres who received microUS to determine whether a biopsy was warranted is currently being analysed to provide initial evidence supporting the use of microUS in a screening setting[81].

Conclusions

MicroUS is a promising technology for prostate cancer detection, combining high-resolution imaging with real-time guidance during biopsy procedures, thereby enhancing procedural accuracy, patient convenience and cost-effectiveness. With the publication of the OPTIMUM trial, level 1 evidence is available for the use of microUS to guide biopsy. Currently ongoing trials are aimed at determining the utility of microUS for various indications of prostate imaging such as AS and biopsy avoidance. Inter-reader variability remains an issue, which might be overcome with new versions of the PRI-MUS score or AI-generated overlays.

Published online: 27 November 2025

References

1. Young, H. H. & Davis, D. M. *Young's Practice of Urology, Based on a Study of 12,500 Cases (1926)* book review. *Ind. Med. Gaz.* **62**, 350–351 (1927).
2. Shinohara, K., Master, V. A., Chi, T., Carroll, P. R. in *Comprehensive Textbook of Genitourinary Oncology* (eds Vogelzang, N. J. et al.) 111–119 (Lippincott, Williams & Wilkins, 2006).
3. Astraldi, A. Diagnosis of cancer of the prostate; biopsy by rectal route. *Urol. Cutan. Rev.* **41**, 421–427 (1937).
4. Peirson, E. L. & Nickerson, D. A. Biopsy of the prostate with the Silverman needle. *N. Engl. J. Med.* **228**, 675–678 (1943).
5. Grabstald, H. Biopsy techniques in the diagnosis of cancer of the prostate. *CA Cancer J. Clin.* **15**, 134–138 (1965).
6. Kaufman, J. J., Rosenthal, M. & Goodwin, W. E. Needle biopsy in diagnosis of prostatic cancer. *Calif. Med.* **81**, 308 (1954).
7. Takahashi, H. & Ouchi, T. The ultrasonic diagnosis in the field of urology. *Proc. Jpn. Soc. Ultrason. Med.* **3**, 7 (1963).
8. Watanabe, H., Igari, D., Tanahasi, Y., Harada, K. & Saitoh, M. Development and application of new equipment for transrectal ultrasonography. *J. Clin. Ultrasound* **2**, 91–98 (1974).
9. Hodge, K. K., McNeal, J. E. & Stamey, T. A. Ultrasound guided transrectal core biopsies of the palpably abnormal prostate. *J. Urol.* **142**, 66–70 (1989).
10. Kwon, E. D. & Williams, R. D. Magnetic resonance imaging in the evaluation of prostate cancer. *World J. Urol.* **7**, 17–21 (1989).
11. Giganti, F. et al. The evolution of MRI of the prostate: the past, the present, and the future. *Am. J. Roentgenol.* **213**, 384–396 (2019).
12. Turkbey, B. et al. Prostate imaging reporting and data system version 2.1: 2019 update of prostate imaging reporting and data system version 2. *Eur. Urol.* **76**, 340–351 (2019).
13. Barentsz, J. O. et al. ESUR prostate MR guidelines 2012. *Eur. Radiol.* **22**, 746–757 (2012).
14. Cornford, P. et al. EAU-EANM-ESTRO-ESUR-ISUP-SIOG Guidelines on Prostate Cancer — 2024 Update. Part I: screening, diagnosis, and local treatment with curative intent. *Eur. Urol.* **86**, 148–163 (2024).
15. Borofsky, S. et al. What are we missing? False-negative cancers at multiparametric MR imaging of the prostate. *Radiology* **286**, 186–195 (2018).
16. Kinnaird, A. et al. Risk of prostate cancer after a negative magnetic resonance imaging guided biopsy. *J. Urol.* **204**, 1180–1186 (2020).
17. Emmett, L. et al. The PRIMARY Score: using intraprostatic 68Ga-PSMA PET/CT patterns to optimize prostate cancer diagnosis. *J. Nucl. Med.* **63**, 1644–1650 (2022).
18. Mookerji, N. et al. Fluorine-18 prostate-specific membrane antigen-1007 PET/CT vs multiparametric MRI for locoregional staging of prostate cancer. *JAMA Oncol.* **10**, 1097–1103 (2024).
19. Kinnaird, A. et al. Microultrasonography-guided vs MRI-guided biopsy for prostate cancer diagnosis: the OPTIMUM randomized clinical trial. *JAMA* **333**, 1679–1687 (2025).
20. Sherar, M. D., Noss, M. B. & Foster, F. S. Ultrasound backscatter microscopy images the internal structure of living tumour spheroids. *Nature* **330**, 493–495 (1987).
21. Pavlin, C. J., Sherar, M. D. & Foster, F. S. Subsurface ultrasound microscopic imaging of the intact eye. *Ophthalmology* **97**, 244–250 (1990).
22. Pavlin, C. J., Harasiewicz, K., Sherar, M. D. & Foster, F. S. Clinical use of ultrasound biomicroscopy. *Ophthalmology* **98**, 287–295 (1991).
23. Hoffmann, K., El Gammal, S., Matthes, U. & Altmeyer, P. Digital 20 MHz sonography of the skin in preoperative diagnosis. *Z. Hautkr.* **64**, 851–852 (1989).
24. Hoffmann, K., El Gammal, S. & Altmeyer, P. B-scan ultrasound in dermatology. *Hautarzt* **41**, W7–W16 (1990).
25. Nissen, S. E. et al. Application of a new phased-array ultrasound imaging catheter in the assessment of vascular dimensions: in vivo comparison to cineangiography. *Circulation* **81**, 660–666 (1990).
26. Bom, N., ten Hoff, H., Lancée, C. T., Gussenhoven, W. J. & Bosch, J. G. Early and recent intraluminal ultrasound devices. *Int. J. Card. Imaging* **4**, 79–88 (1989).
27. Turnbull, D. H., Bloomfield, T. S., Baldwin, H. S., Foster, F. S. & Joyner, A. L. Ultrasound backscatter microscope analysis of early mouse embryonic brain development. *Proc. Natl. Acad. Sci. USA* **92**, 2239 (1995).
28. Foster, F. S. et al. A new ultrasound instrument for in vivo microimaging of mice. *Ultrasound Med. Biol.* **28**, 1165–1172 (2002).
29. Foster, F. S., Pavlin, C. J., Harasiewicz, K. A., Christopher, D. A. & Turnbull, D. H. Advances in ultrasound biomicroscopy. *Ultrasound Med. Biol.* **26**, 1–27 (2000).
30. Foster, F. S. et al. A new 15–50 MHz array-based micro-ultrasound scanner for preclinical imaging. *Ultrasound Med. Biol.* **35**, 1700–1708 (2009).
31. Wirtzfeld, L. A. et al. A new three-dimensional ultrasound microimaging technology for preclinical studies using a transgenic prostate cancer mouse model. *Cancer Res.* **65**, 6337–6345 (2005).
32. Graham, K. C. et al. Three-dimensional high-frequency ultrasound imaging for longitudinal evaluation of liver metastases in preclinical models. *Cancer Res.* **65**, 5231–5237 (2005).
33. Xuan, J. W. et al. Functional neoangiogenesis imaging of genetically engineered mouse prostate cancer using three-dimensional power Doppler ultrasound. *Cancer Res.* **67**, 2830–2839 (2007).
34. Franco, M. et al. Targeted anti-vascular endothelial growth factor receptor-2 therapy leads to short-term and long-term impairment of vascular function and increase in tumor hypoxia. *Cancer Res.* **66**, 3639–3648 (2006).
35. Pavlovich, C. P. et al. High-resolution transrectal ultrasound: pilot study of a novel technique for imaging clinically localized prostate cancer. *Urol. Oncol.* **32**, 34.e27–34.e32 (2014).
36. Pavlovich, C. P. et al. A multi-institutional randomized controlled trial comparing first-generation transrectal high-resolution micro-ultrasound with conventional frequency transrectal ultrasound for prostate biopsy. *BJUI Compass* **2**, 126–133 (2021).
37. Lughezzani, G. et al. Comparison of the diagnostic accuracy of micro-ultrasound and magnetic resonance imaging/ultrasound fusion targeted biopsies for the diagnosis of clinically significant prostate cancer. *Eur. Urol. Oncol.* **2**, 329–332 (2019).
38. Claros, O. R. et al. Comparison of initial experience with transrectal magnetic resonance imaging cognitive guided micro-ultrasound biopsies versus established transperineal robotic ultrasound magnetic resonance imaging fusion biopsies for prostate cancer. *J. Urol.* **203**, 918–923 (2020).
39. Klotz, L. et al. Comparison of micro-ultrasound and multiparametric magnetic resonance imaging for prostate cancer: a multicenter, prospective analysis. *Can. Urol. Assoc. J.* **15**, E11–E16 (2020).
40. Lughezzani, G. et al. Diagnostic accuracy of microultrasound in patients with a suspicion of prostate cancer at magnetic resonance imaging: a single-institutional prospective study. *Eur. Urol. Focus* **7**, 1019–1026 (2021).
41. Avolio, P. P. et al. Enhanced diagnostic accuracy of micro-ultrasound in prostate cancer detection: an updated series from a single-center prospective study. *Urol. Oncol.* **43**, 470.e19–470.e26 (2025).
42. Wiemer, L. et al. Evolution of targeted prostate biopsy by adding micro-ultrasound to the magnetic resonance imaging pathway. *Eur. Urol. Focus.* **7**, 1292–1299 (2021).
43. Hofbauer, S. L. et al. A non-inferiority comparative analysis of micro-ultrasonography and MRI-targeted biopsy in men at risk of prostate cancer. *BJU Int.* **129**, 648–654 (2022).
44. Ghai, S. et al. Comparison of micro-US and multiparametric MRI for prostate cancer detection in biopsy-naive men. *Radiology* **305**, 390–398 (2022).
45. Avolio, P. P. et al. The use of 29 MHz transrectal micro-ultrasound to stratify the prostate cancer risk in patients with PI-RADS III lesions at multiparametric MRI: a single institutional analysis. *Urol. Oncol.* **39**, 832.e1–832.e7 (2021).
46. Albers, P. et al. Micro-ultrasound for the detection of clinically significant prostate cancer in biopsy-naive men with negative MRI. *Can. Urol. Assoc. J.* **18**, 208–211 (2024).
47. Avolio, P. P. et al. Assessing the role of high-resolution microultrasound among naïve patients with negative multiparametric magnetic resonance imaging and a persistently high suspicion of prostate cancer. *Eur. Urol. Open. Sci.* **47**, 73–79 (2023).
48. Beatrici, E. et al. Optimizing prostate cancer diagnostic work-up through micro-ultrasound: minimizing unnecessary procedures and reducing overdiagnoses. *Prostate* **85**, 603–611 (2025).
49. James, N. D. et al. The lancet commission on prostate cancer: planning for the surge in cases. *Lancet* **403**, 1683–1722 (2024).
50. Richemond, A. et al. Predicting pathological tumor volume in prostate cancer lesions: a head-to-head comparison of micro-ultrasound vs. MRI. *Urol. Oncol.* **43**, 398. e15–398.e21 (2025).
51. Pensa, J. et al. Evaluation of prostate cancer detection using micro-ultrasound versus MRI through co-registration to whole-mount pathology. *Sci. Rep.* **14**, 18910 (2024).
52. Ghai, S. et al. Assessing cancer risk on novel 29 MHz micro-ultrasound images of the prostate: creation of the micro-ultrasound protocol for prostate risk identification. *J. Urol.* **196**, 562–569 (2016).
53. Schaer, S. et al. Assessing cancer risk in the anterior part of the prostate using micro-ultrasound: validation of a novel distinct protocol. *World J. Urol.* **41**, 3325 (2023).

54. Pedraza, A. M. et al. Microultrasound in the detection of the index lesion in prostate cancer. *Prostate* **84**, 79–86 (2024).
55. Zhou, S. R. et al. Inter-reader agreement for prostate cancer detection using micro-ultrasound: a multi-institutional study. *Eur. Urol. Open Sci.* **66**, 93–100 (2024).
56. Lu, A. J. et al. Role of core number and location in targeted magnetic resonance imaging-ultrasound fusion prostate biopsy. *Eur. Urol.* **76**, 14–17 (2019).
57. Albers, P. et al. Value of incremental biopsy cores for microultrasound targeted prostate biopsies. *Urology* **184**, 142–148 (2024).
58. Cash, H. et al. Prostate cancer detection by novice micro-ultrasound users enrolled in a training program. *Soc. Int. Urol. J.* **3**, 62–68 (2022).
59. Eure, G., Fanney, D., Lin, J., Wodlinger, B. & Ghai, S. Comparison of conventional transrectal ultrasound, magnetic resonance imaging, and micro-ultrasound for visualizing prostate cancer in an active surveillance population: a feasibility study. *Can. Urol. Assoc. J.* **13**, E70 (2018).
60. Maffei, D. et al. Diagnostic performance of microUltrasound at MRI-guided confirmatory biopsy in patients under active surveillance for low-risk prostate cancer. *Prostate* **83**, 886–895 (2023).
61. Albers, P. et al. Micro-ultrasound versus magnetic resonance imaging in prostate cancer active surveillance. *Eur. Urol. Open Sci.* **46**, 33–35 (2022).
62. Regis, F. et al. Use of 29-MHz Micro-ultrasound for local staging of prostate cancer in patients scheduled for radical prostatectomy: a feasibility study. *Eur. Urol. Open Sci.* **19**, 20–23 (2020).
63. Fasulo, V. et al. Use of high-resolution micro-ultrasound to predict extraprostatic extension of prostate cancer prior to surgery: a prospective single-institutional study. *World J. Urol.* **40**, 435–442 (2022).
64. Staerman, F. Can high resolution micro-ultrasound detect extra-prostatic extension? A new sonographic feature. *Eur. Urol. Suppl.* **17**, e2762 (2018).
65. Lehto, T. P. K. et al. Histomic and transcriptomic features of MRI-visible and invisible clinically significant prostate cancers are associated with prognosis. *Int. J. Cancer* **154**, 926–939 (2024).
66. Cornud, F. et al. MRI-directed micro-US-guided transperineal focal laser ablation for localized prostate cancer: a 1-year follow-up study. *Radiology* **313**, e233371 (2024).
67. Stanton, W., Crawford, E. D., Arangua, P., Hoyer, G. & Werahera, P. N. Evaluation of the 29Mhz micro-ultrasound imaging for prostate cancer diagnosis and treatment. *Ann. Urol. Nephrol.* **1**, AUN.2020.01.000515 (2019).
68. Jiang, H. et al. MicroSegNet: a deep learning approach for prostate segmentation on micro-ultrasound images. *Comput. Med. Imaging Graph.* **112**, 102326 (2024).
69. Gilany, M. et al. TRUSformer: improving prostate cancer detection from micro-ultrasound using attention and self-supervision. *Int. J. Comput. Assist. Radiol. Surg.* **18**, 1193–1200 (2023).
70. Harmanani, M. et al. TRUSWorthy: toward clinically applicable deep learning for confident detection of prostate cancer in micro-ultrasound. *Int. J. Comput. Assist. Radiol. Surg.* **20**, 981–989 (2025).
71. Pensa, J. et al. Deep learning classification of prostate cancer on confidently labeled micro-ultrasound images. *Annu. Int. Conf. IEEE Eng. Med. Biol. Soc. 2024* https://doi.org/10.1109/EMBC53108.2024.10782375 (2024).
72. Wilson, P. F. R. in Linguraru, M. G. (ed). *Medical Image Computing and Computer Assisted Intervention* – MICCAI 2024 (ed. Linguraru, M. G.) 499–509 (Springer, 2024).
73. Zhou, S. R. et al. ProMUS-NET: Artificial intelligence detects more prostate cancer than urologists on micro-ultrasonography. *BJU Int.* **136**, 1071–1079 (2025).
74. Saita, A. et al. Assessing the feasibility and accuracy of high-resolution microultrasound imaging for bladder cancer detection and staging. *Eur. Urol.* **77**, 727–732 (2020).
75. Diana, P. et al. Head-to-head comparison between high-resolution microultrasound imaging and multiparametric MRI in detecting and local staging of bladder cancer: the bus-miss protocol. *Bladder Cancer* **8**, 119–127 (2022).
76. Huang, D. Y. et al. Multiparametric ultrasound for focal testicular pathology: a ten-year retrospective review. *Cancers* **16**, 2309 (2024). 2024;16:2309.
77. US National Library of Medicine. *ClinicalTrials.gov* https://clinicaltrials.gov/study/NCT06941922 (2025).
78. Frankiewicz, M. et al. Ultrasound imaging of male urethral stricture disease: a narrative review of the available evidence, focusing on selected prospective studies. *World J. Urol.* **42**, 32 (2024).
79. US National Library of Medicine. *ClinicalTrials.gov* https://clinicaltrials.gov/study/NCT05558241 (2025).
80. US National Library of Medicine. *ClinicalTrials.gov* https://www.clinicaltrials.gov/study/NCT06626022 (2025).
81. German Clinical Trials Register. https://drks.de/search/en/trial/DRKS00036777 (2025).

Author contributions

A.K. and M.G. researched data for the article. A.K. and M.G. contributed substantially to discussion of the content. A.K., M.G., L.K. and P.F.R.W. wrote the article. All authors reviewed and/or edited the manuscript before submission.

Competing interests

The authors declare no competing interests.

Additional information

Peer review information *Nature Reviews Urology* thanks Massimo Lazzeri and the other, anonymous, reviewer(s) for their contribution to the peer review of this work.

Publisher's note Springer Nature remains neutral with regard to jurisdictional claims in published maps and institutional affiliations.

Springer Nature or its licensor (e.g. a society or other partner) holds exclusive rights to this article under a publishing agreement with the author(s) or other rightsholder(s); author self-archiving of the accepted manuscript version of this article is solely governed by the terms of such publishing agreement and applicable law.

© Springer Nature Limited 2025